Seam Welding of Aluminum Sheet Using Ultrasonic Additive Manufacturing System

Paul J. Wolcott
Center for Ultrasonic Additive Manufacturing,
The Ohio State University,
Columbus, OH 43210
e-mail: wolcott.27@osu.edu

Christopher Pawlowski
Center for Ultrasonic Additive Manufacturing,
The Ohio State University,
Columbus, OH 43210
e-mail: pawlowski.24@osu.edu

Leon M. Headings
Center for Ultrasonic Additive Manufacturing,
The Ohio State University,
Columbus, OH 43210
e-mail: headings.4@osu.edu

Marcelo J. Dapino[1]
Center for Ultrasonic Additive Manufacturing,
The Ohio State University,
Columbus, OH 43210
e-mail: dapino.1@osu.edu

Ultrasonic welding was investigated as a method of joining 0.076 in. (1.93 mm) thick aluminum 6061 flat sheet material. Joints were produced with ultrasonic additive manufacturing (UAM) equipment in a modified application of the ultrasonic welding process. Through joint design development, successful welds were achieved with a scarf joint configuration. Using a design of experiments (DOE) approach, weld parameters including weld amplitude, scarf angle, and weld speed were optimized for mechanical strength. Lower angles and higher amplitudes were found to provide the highest strengths within the levels tested. Finite-element studies indicate that 5 deg and 10 deg angles produce an increased relative motion of the workpieces as compared to 15 deg, 20 deg, and 25 deg angles, likely leading to increased strength. Successful joints showed no indication of voids under optical microscopy. As-welded joints produce tensile strengths of 221 MPa, while heat treated joints produce tensile strengths of 310 MPa, comparable to heat treated bulk material. High-temperature tensile testing was conducted at 210 °C, with samples exhibiting strengths of 184.1 MPa, similar to bulk material. Room temperature fatigue testing resulted in cyclic failures at approximately 190,000 cycles on average, approaching that of bulk material. [DOI: 10.1115/1.4034007]

Keywords: ultrasonic seam welding, ultrasonic additive manufacturing, sheet metal joining, aluminum, heat treatment, fatigue

1 Introduction

Sheet materials are used extensively applications in automotive, aerospace, marine, and other industries. Joining these materials to one another for integration into structures is a key engineering challenge. A variety of techniques exist for joining sheet metals, including rivets, welding, bolts, fasteners, etc. [1]. Rivets and other mechanical fasteners can be prone to corrosion and lower strength in certain conditions [2]. In some instances, rivets or other mechanical fasteners protrude from the surface of the sheet metal. This protrusion can affect flow characteristics in applications involving fluid flow over the sheet, making them prohibitive in specific applications [3]. Flush rivets can eliminate this protrusion but cannot be applied in all joint geometries due to access requirements for in situ non-destructive evaluation (NDE) inspections.

Seam welds with a flush surface finish can be achieved with alternative welding processes such as fusion welding; however, the heat-affected zone can degrade the mechanical properties of the material by altering the microstructure [4]. Age-hardenable materials such as 6xxx series aluminum are prone to such weakening. Heating of these materials can solutionize or grow the precipitates that provide strengthening, leading to a significantly weaker material in the heat-affected zone [5]. This heat-affected zone can reduce strengths on the order of 30–50% and can extend between 10 mm and 30 mm from the weld centerline [6]. Solid state techniques, such as ultrasonic welding and impact welding, can reduce the degradation in properties since their process temperatures are well below melting of the constituent materials and the bond affected zone is much smaller, on the order of 15 μm [7–9].

Techniques that fall in the overall category of ultrasonic metal welding, such as UAM and ultrasonic seam welding, are capable of creating a flush joint configuration without significant heating [10,11]. The UAM process involves additive welding of metal foils, typically 0.006 in. (0.152 mm) thick, which are successively layered until a desired geometry is attained [12]. Conceptually, this technique could be applied to join sheet structures, however, not as efficiently as techniques such as ultrasonic seam welding that directly join the sheets in a single pass. Existing ultrasonic seam and spot welding techniques have been unable to apply the necessary weld power through material motion required to join alloyed aluminum at 0.076 in. (1.93 mm) thickness. The concept presented here utilizes a 9 kW UAM machine to perform ultrasonic seam welding for joining aluminum 6061-T6 sheet metal 0.076 in. (1.93 mm) thick. This is a nontraditional application of the UAM framework, expanding the capabilities and potential applications of the technology. The nominal composition of Al 6061 is given in Table 1. An example schematic of the concept is presented in Fig. 1. Aluminum 6061 was chosen because it is a common alloy in many applications; however, the joint design developments in this study could be applied to other material systems as well. This work examines the design of sheet metal joints utilizing UAM equipment through characterization of their room temperature and elevated temperature tensile strength, as well as their room temperature fatigue properties.

The originality of this paper comes from the utilization of UAM equipment to produce seam welds at higher thicknesses, with higher strengths, and in a joint design that has not been examined using other ultrasonic processes. Utilizing this process, flush seam joints can be created with mechanical properties similar to bulk Al 6061-T6. Additionally, while not discussed in this paper, the UAM process would allow for the additive production of near-net shape features on existing structures along with the sheet joining methodology presented here.

Table 1 Nominal composition of Al 6061 [13]

Mg	Si	Cu	Cr	Al
1%	0.6%	0.30%	0.20%	Balance

[1]Corresponding author.

Manuscript received April 27, 2015; final manuscript received June 20, 2016; published online August 15, 2016. Assoc. Editor: Wayne Cai.

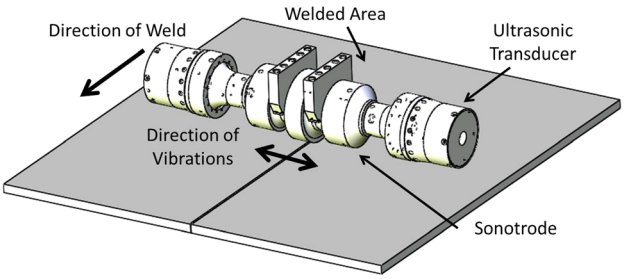

Fig. 1 Concept for using a UAM welder to join two metal sheets

2 Joint Design

2.1 Thickness Scoping. To begin the design of a sheet metal joint using ultrasonic welding, it is necessary to determine the weldable thickness range. Existing state-of-the-art for UAM built structures uses foils on the order of 0.006 in. (0.152 mm) thick [12], while ultrasonic seam welding of 1100 aluminum alloys has been successfully conducted on 0.3 mm thick material [14]. The goal of pilot testing is to determine the maximum weld thickness possible, identifying the envelope of geometries for joint design. Pilot test welds were performed to determine the weldable envelope for Al 6061-T6 employing a range of foil thicknesses including 0.006 (0.152), 0.016 (0.406), 0.020 (0.508), 0.025 (0.635), 0.030 (0.762), 0.032 (0.813), and 0.035 (0.889) in. (mm). The strips were ultrasonically welded to an aluminum 6061-T6 baseplate using a Fabrisonic SonicLayer 4000 UAM system. An image of a trial using 0.016 in. (0.406 mm) thick aluminum is shown in Fig. 2 where the foil, textured by the sonotrode during welding, and the baseplate are shown. The test welds were performed at room temperature with a foil width of 0.5 in. (1.27 mm). A successful weld was determined as one which stuck to the baseplate and could not be easily peeled off manually, while also not welding directly to the sonotrode. All welds were performed with a 7 μm R_a roughness sonotrode. Weld parameters including welder vibration amplitude, weld speed, and weld force were varied until a weld was achieved or it was clear that a weld was not possible at that thickness. A maximum thickness of 0.032 in. (0.813 mm) was identified as viable. Attempts to exceed this thickness resulted in inadequate welding or direct welding to the sonotrode. The weld parameters for the 0.032 in. (0.813 mm) thickness pilot welds are shown in Table 2. These parameters indicate levels at which a weld can be achieved, but do not represent an optimized set.

2.2 Development of Joint Configuration. Using the parameters developed for the maximum weld thickness of 0.032 in. (0.813 mm), a lap joint was designed to join sheet material 0.063 in. (1.6 mm) thick. This thickness is roughly twice the maximum thickness identified as weldable. The joint design is a lap configuration consisting of two separately machined sheets, with matching steps that are welded over to create the joint. A schematic of the lap joint configuration is shown in Fig. 3(*a*). The channels denoted in the figure were machined into the sheet to control the horn contact area during development. In a production application, the horn width would be designed to eliminate the need for channels. The sheets were fixed in place with a vacuum chuck.

Reasonably successful joints can be achieved with the lap joint design. Specifically, there are no indications of voids in the horizontal portion of the joint, but there is a lack of bonding in the vertical portions, as shown in the cross section in Fig. 3(*b*). It is expected that the imperfect bonding is due to the lack of relative sliding motion and normal force between the two sheets in those areas. Because the ultrasonic vibrations are applied normal to the mating vertical surfaces, scrubbing does not occur, which is necessary for bonding. Therefore, in order to achieve complete bonding, the joint design must allow relative sliding motion between all mating surfaces.

Following these principles, other joint designs were considered. Of specific interest are angled scarf joint configurations that allow the mating surfaces to move relative to one another while remaining relatively simple to manufacture. To test this concept, a joint was created with an angle on one side and a lap joint mating on the other. The joint schematic and a cross section of the joint are shown in Fig. 4. While voids are present around the vertical mating surfaces, there are no voids in the angled portion of the joint. This indicates that the angle allows sufficient relative scrubbing action for joining to occur.

Based on the successful welding of angled surfaces, the angled joint concept was applied to the full joint thickness, as shown in Fig. 5(*a*) for an Al 6061-T6 scarf joint with 0.076 in. (1.93 mm) thickness. Once again, channels were machined on both sides of the joint to control the horn contact area.

Due to the presence of voids in the scarf joint, as shown in Fig. 5(*b*), the use of a second weld pass was considered. Initially, two weld passes were attempted on the same side of the joint. This approach produced voids at the bottom of the joint, likely due to limited relative motion at this location. A better bond was

Table 2 Welding parameters for 0.032 in. (0.8128 mm) thick Al 6061-T6 foil with 0.5 in. (12.7 mm) width

Process variable	Set value
Weld normal force (N)	1500
Weld speed (in./min) (mm/s)	30 (12.7)
Amplitude (μm)	41.4
Spot time (ms)	225
Sonotrode surface texture, R_a (μm)	7
Oscillation frequency (kHz)	20

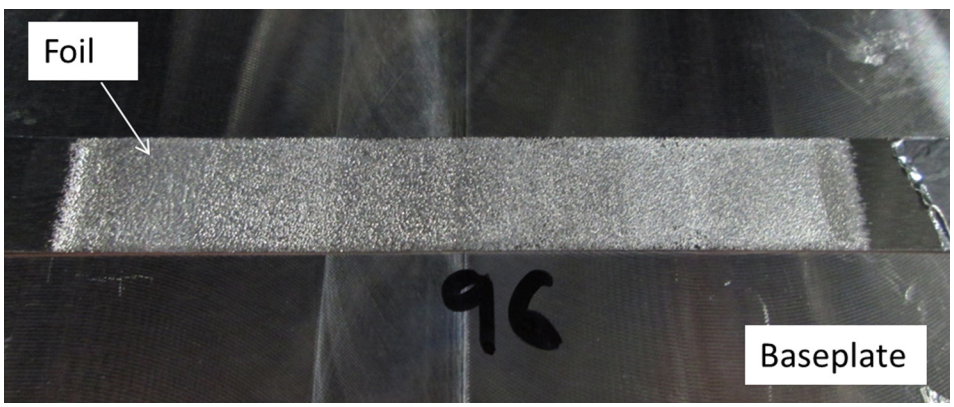

Fig. 2 Image of 0.016 in. (0.406 mm) thickness scoping trial for Al 6061

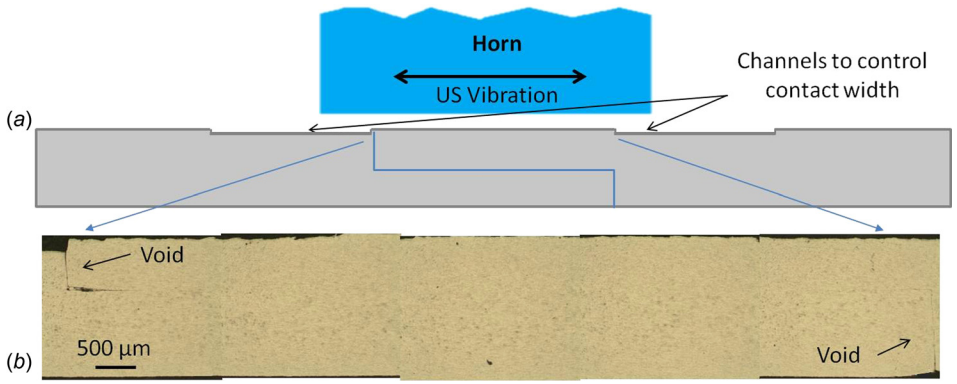

Fig. 3 Lap joint (*a*) schematic and (*b*) cross section

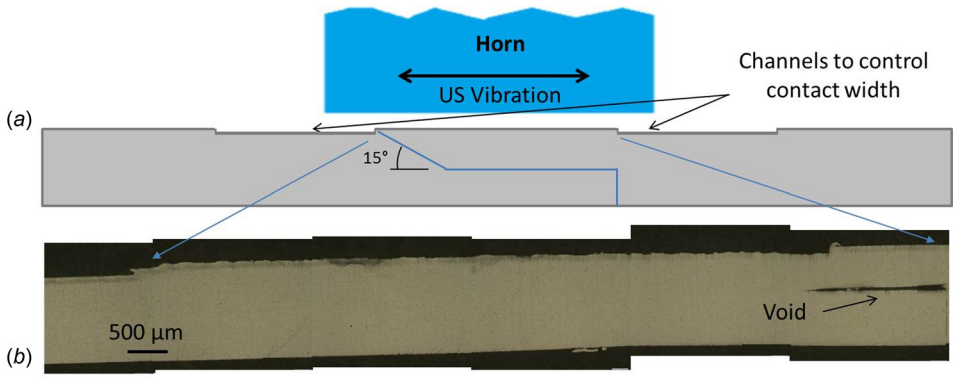

Fig. 4 Angled lap joint (*a*) schematic and (*b*) cross section

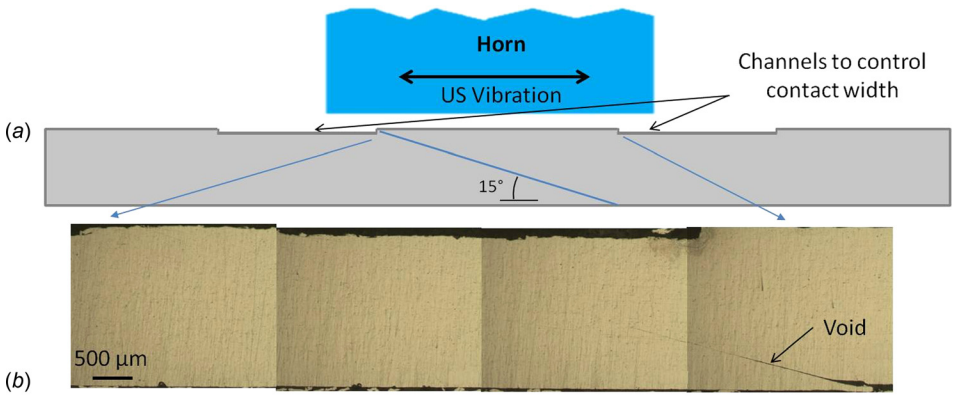

Fig. 5 Scarf joint (*a*) schematic and (*b*) cross section

achieved by turning the sheet over after the initial weld pass and performing a second weld pass on the opposite side of the joint, as illustrated in Fig. 6(*a*). Figure 6(*b*) shows the cross section of a scarf joint that was welded from both sides. In this case, there are no apparent voids along the length of the joint; the faint lines in the image are an artifact of the polishing process.

2.3 Design of Experiments (DOE) Study. A lack of voids does not guarantee maximum strength for the joint. Therefore, a design of experiments (DOE) study was conducted to gain a better understanding of the effects of welder vibration amplitude, weld speed, and weld angle on joint strength. This study investigated five different weld angles, two levels of horn vibration amplitude, and two weld speeds for a scarf joint with welding on both sides of 0.076 in. (1.931 mm) thick Al 6061-T6 sheet. The experimental design is shown in Table 3. For a constant joint thickness, if the angle varies, the width of the weld varies significantly, from 20.574 mm at 5 deg to 4.191 mm at 25 deg. Therefore, a constant normal force would apply varying levels of pressure to mating joint surfaces, confounding the process parameters being examined. To keep the pressure constant for different angles, the applied normal force was varied based on the joint width. Additionally, the relative vibration amplitude applied along the mating joint surfaces changes with angle according to a cosine relationship. For this reason, the amplitude was also compensated based on the angle. The compensated weld parameters are provided in Table 4.

To conduct the DOE, ultrasonically welded joints were manufactured for each of the parameters outlined in Table 4. Tensile tests were performed on the constructed joints using an Interlaken load frame with a 0.05 in./min (0.02 mm/s) displacement rate. All

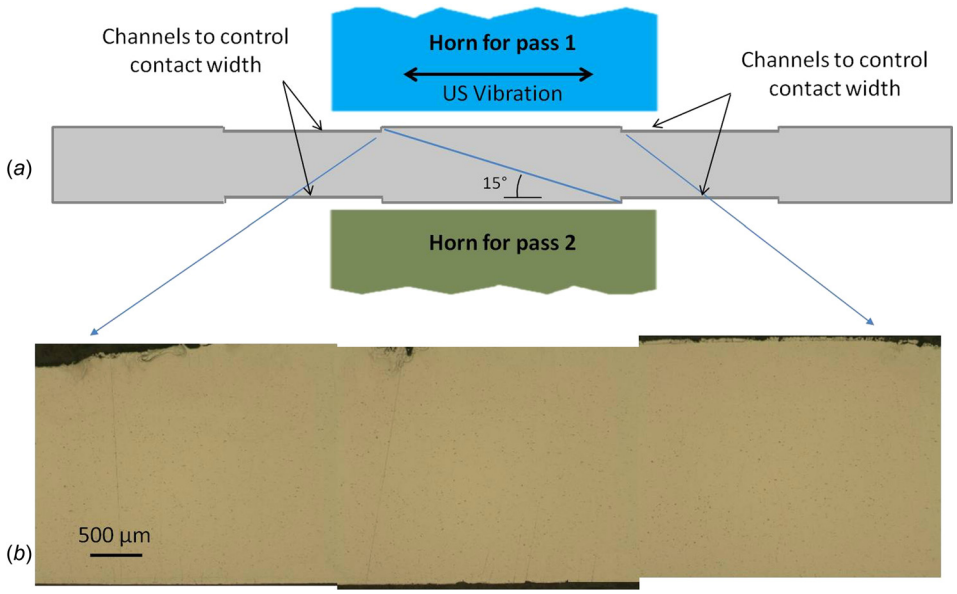

Fig. 6 Scarf joint with welding on both sides: (*a*) schematic and (*b*) cross section

Table 3 DOE for angle, amplitude, and weld speed

Angle (deg)	Amplitude	Weld speed (in./min) (mm/s)
5	High, low	29 (12.28), 25 (10.58)
10	High, low	29 (12.28), 25 (10.58)
15	High, low	29 (12.28), 25 (10.58)
20	High, low	29 (12.28), 25 (10.58)
25	High, low	29 (12.28), 25 (10.58)

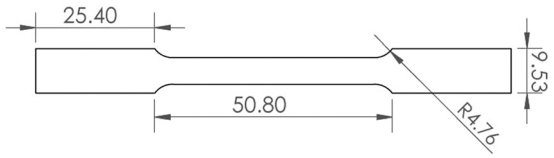

Fig. 7 Test specimen geometry for tensile testing (dimensions are in millimeters), with 0.065 in. (1.651 mm) thickness

samples were machined to a uniform thickness of 0.065 in. (1.651 mm), removing the channels machined during joint manufacturing, followed by machining to final dimensions. The sample dimensions are shown in Fig. 7.

2.4 Analysis of DOE. Following the DOE, statistical analyses, including analysis of variance (ANOVA), were conducted on the resulting data. ANOVA is used to compare three or more variables for their statistical significance on an examined process. The analysis uses a generalized linear model to describe the behavior, with the following form:

$$Y_{ijkt} = \mu + \alpha_i + \beta_j + \gamma_k + \varepsilon_{ijkt} \quad (1)$$

The linear equation (1) describes the dependence of the response variable Y on the various treatment factors. In this case, Y is the tensile strength and μ represents the overall mean of Y. The treatment factors α_i, β_j, and γ_k represent the main effects of the process parameters, with α_i denoting the effect of angle at the ith level while the other factors are fixed, β_j representing the effect of amplitude at the jth level, and γ_k representing the effect of weld speed at the kth level. The error variable ε represents any nuisance response in the model and exhibits a normal distribution with zero mean. All ε_{ijkt} are mutually independent with respect to i, j, k, and t.

Table 5 ANOVA table for tensile strength

Source	DF	Seq. SS	Adj. SS	Adj. MS	F	p-value
Angle	4	1860.76	1860.76	465.19	49.26	<0.001
Amplitude	1	116.47	116.47	116.47	12.33	0.001
Speed	1	0.04	0.04	0.04	0	0.946
Error	53	500.55	500.55	9.44	—	—
Total	59	2477.8				

The ANOVA results for tensile strength are shown in Table 5. In the ANOVA table, the p-value represents the probability of obtaining a result at least as extreme as the observation, under the assumption that a null hypothesis of no effect is true. Lower p-values are indicative of stronger evidence against the null hypothesis. In this study, p-values of < 0.05 are considered indicative of significant evidence against the null hypothesis. As shown in Table 5, p-values for both angle and amplitude are < 0.05, indicating that the angle and amplitude have significant effects on ultimate tensile strength (UTS), while weld speed with a p-value of

Table 4 Compensated weld parameters for low and high levels of amplitude

Angle (deg)	Horn contact width (mm)	Weld force (N)	Low amplitude (μm)	High amplitude (μm)
5	20.574	5759	38.0	40.0
10	11.100	2924	38.5	40.4
15	7.290	2000	39.2	41.2
20	5.385	1556	40.3	42.4
25	4.191	1305	41.8	43.9

0.946 does not have a significant effect over the range of speeds tested. This study focuses on main effects since two-factor interactions were found to be negligible, though this analysis is not included for brevity. This result agrees with the previous studies on ultrasonic joining where interaction effects in process parameters were largely insignificant [15–17].

The main effects plots shown in Fig. 8 reinforce these conclusions. In each plot, lower levels for angle yield higher levels of tensile strength. Likewise, for amplitude, high levels of amplitude lead to higher levels of tensile strength.

Optimal conditions for strength can be determined using Tukey pairwise comparisons to evaluate the significance of variation from one level to the next [18]. These are comparisons between the various levels of angle and amplitude, comparing the significance of variation from one level to the next [18]. The comparison follows the equation

$$\tau_i - \tau_s \in (\bar{y}_i - \bar{y}_s) \pm \omega_T \sqrt{ms\mathrm{E}\left(\frac{1}{r_i} + \frac{1}{r_s}\right)} \tag{2}$$

where ω_T is taken from a studentized distribution depending on the dataset. When interpreting Tukey pairwise comparison tables, if a comparison range from the lower to higher value includes zero, it is not considered statistically significant. If the comparison range does not include zero, it indicates that a statistically significant difference between two levels is observed at a 95% confidence.

Tukey pairwise comparisons between the levels of angle and amplitude are presented in Tables 6 and 7 for the UTS data. From Table 6, it can be seen that the levels for the 5 deg and 10 deg angles are not statistically different, while the differences between 5 deg and all other angles are significant. Because there is no statistically significant difference between 5 deg and 10 deg, this study indicates that either of these angles is acceptable for maximizing mechanical strength. Pairwise comparisons for the two levels of amplitude, as shown in Table 7, confirm the ANOVA results that the low and high levels are statistically different.

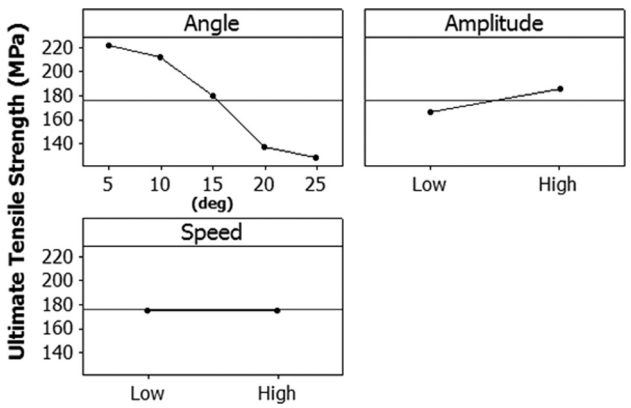

Fig. 8 Main effects plots for UTS

Table 6 Tukey 95% pairwise comparisons among levels of angle compared with angle = 5 deg

Angle (deg)	Lower	Center	Upper
10	−5.07	−1.53	2.01
15	−9.66	−6.12	−2.58
20	−15.99	−12.45	−8.91
25	−17.32	−13.78	−10.24

Table 7 Tukey 95% pairwise comparisons among levels of amplitude compared with low level of amplitude

Amplitude	Lower	Center	Upper
High	1.195	2.786	4.378

Table 8 Optimal levels for scarf joint welding as determined by the DOE study for 0.076 in. (1.931 mm) thick Al 6061-T6 sheet

Process variable	Set value
Weld normal force (N)	2924
Weld speed (in./min) (mm/s)	25 (10.58)
Amplitude (μm)	41
Angle (deg)	10

Based on the results and analyses of the DOE study, the best weld parameters for these joints are presented in Table 8. A 10 deg scarf joint angle was selected because its strength was statistically equivalent to the 5 deg joint angle while being easier to machine. Of note, these are optimized parameters within the levels tested and may not represent a global optimum.

2.5 Finite-Element Modeling. To better understand the effect of the weld angle on bonding, a finite-element analysis was performed using COMSOL MULTIPHYSICS. To model the physics, one sheet of the joint was modeled using a 2D plane strain approximation. The loading conditions applied are shown in Fig. 9. The weld amplitude is applied via displacement at the top of the sheet, similar to how the weld force is applied. Along the bottom of the sheet, a roller condition is used for the first inch (2.54 cm) away from the angle, and a fixed condition is used after that, representing the fixturing conditions of the vacuum chuck. To simplify the model, a condition of no y-direction displacement is used along the angled weld surface. This simplification emulates the effect of the second sheet, while eliminating the need for contact elements. All five angle conditions were modeled separately, according to the compensated amplitudes and forces used in the DOE study (Table 4).

The model results showing the x-displacement for each condition are presented in Fig. 10. As the angle increases, the location where the displacement decreases moves higher on the angled portion of the joint. Comparison of the 5 deg condition with the 25 deg condition shows this clearly, where the 38 μm contour for the 25 deg case is 0.559 mm from the bottom of the joint while this contour is 0.279 mm from the bottom of the joint for the 5 deg case. Because the ultrasonic welding process is based on relative motion, the differences in relative displacement could explain the differences in void content and strength observed between the various angles.

3 Joint Characterization

Using the optimized values determined via the DOE study (Table 8), scarf joints of 0.076 in. (1.931 mm) thick Al 6061-T6 sheets were welded for mechanical testing. Room temperature tensile tests, high-temperature tensile tests at 210 °C, and room temperature fatigue tests were conducted to characterize the joint strength.

3.1 Room Temperature Tensile Testing. Room temperature tensile tests were performed using an Interlaken load frame, with load measured using a load cell with a 5000 lb (22,241 N) range and displacement measured via the linear variable differential transformer built into the frame. Tests were performed using a displacement rate of 0.05 in./min (0.02 mm/s). Averaged test results for three as-built joints are presented in Table 9. The resulting average tensile strength is 221.3 MPa while the tensile strength of

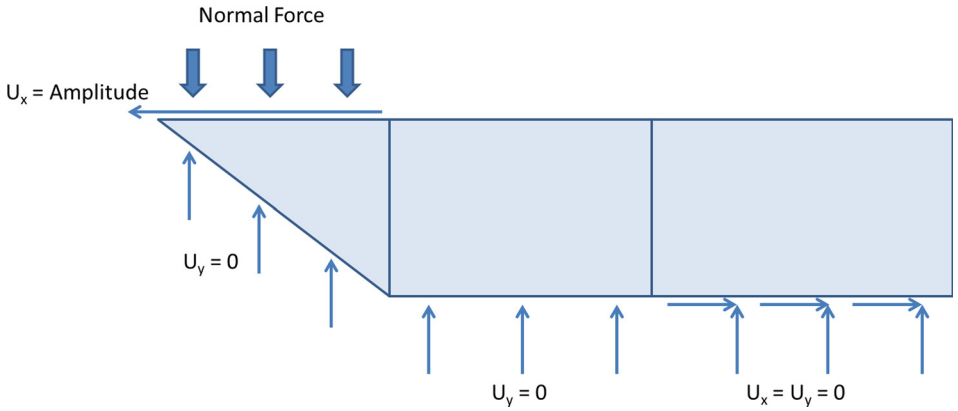

Fig. 9 Boundary conditions and loads applied to FEA model

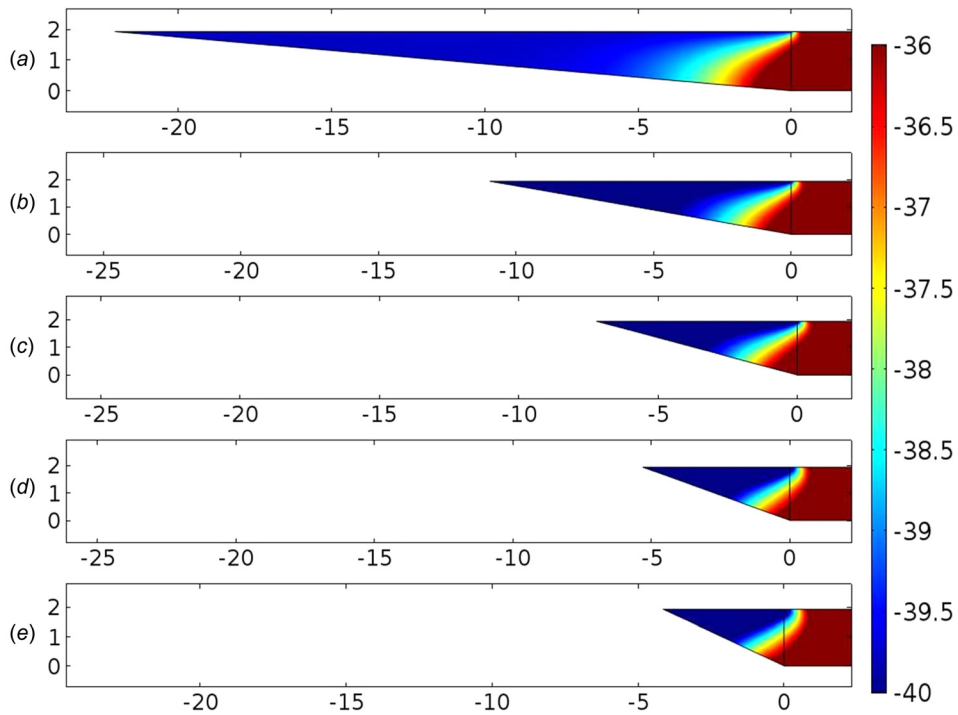

Fig. 10 Horizontal displacement results for each of the five angles modeled: (*a*) 5 deg, (*b*) 10 deg, (*c*) 15 deg, (*d*) 20 deg, and (*e*) 25 deg

Table 9 Room temperature UTS test results for three as-built and heat treated Al 6061 joints

Joint	Avg. UTS (MPa)	SD
As-built	221.3	1.1
Heat treated	311.0	12.2

Table 10 Elevated temperature tensile test results of six heat treated specimens

Sample	Avg. UTS (MPa)	SD	Percentage of bulk RT UTS
Heat treated	184.1	13.0	59.3

bulk aluminum 6061-T6 is 310 MPa [13]. Heat treatments were investigated as a means to improve the tensile properties following joining.

Joint samples were prepared following the T6 treatment for aluminum 6061, by solutionizing at 530 °C then aging at 160 °C for 18 h [19]. Test results for these joints are likewise presented in Table 9. The tensile strength of the heat treated samples increases from an average of 221.3 MPa to 311.0 MPa, matching the bulk material [20]. These results indicate that the tensile strength of the joints can be maximized and that bulk material properties can be achieved using a postprocess heat treatment.

Representative stress–strain data for the as-built and heat treated material are shown in Fig. 11(*a*) and Table 9. Postprocess heat treatments are demonstrated to provide significant enhancements in the tensile strength and elongation. Representative fracture surfaces for the as-built and heat treated samples are presented in Figs. 11(*b*) and 11(*c*). For the as-built sample, failure occurs along the joint, with little ductility, as evidenced by the relatively straight failure line. In contrast, the heat treated sample exhibits much higher ductility, with the failure surface protruding throughout the bond zone and a failure line oriented diagonally through the joint.

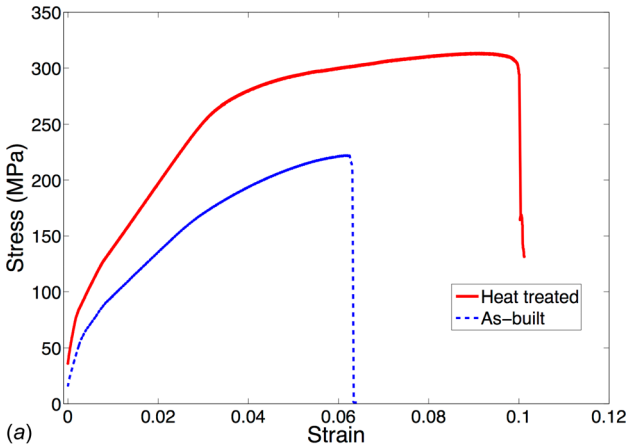

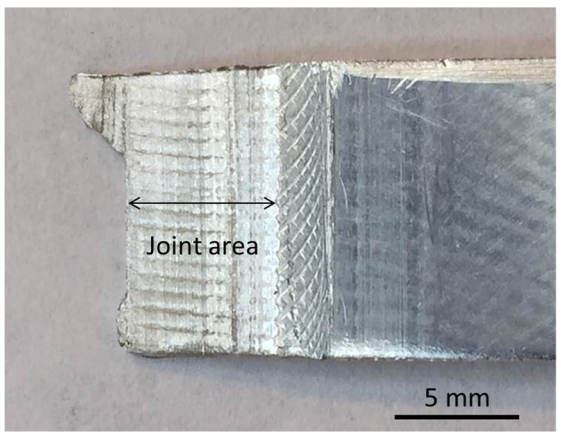

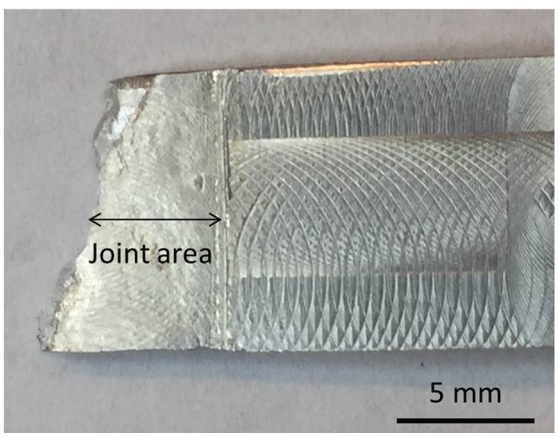

Fig. 11 (*a*) Representative room temperature tensile test results for as-built and heat treated joints, (*b*) fracture surface of as-built joint, and (*c*) fracture surface of heat treated joint

3.2 High-Temperature Tensile Testing. To characterize the high-temperature tensile behavior of the joint, tensile tests were performed at 210 °C within a thermal chamber on a TestResources load frame with a displacement rate of 0.05 in./min (0.02 mm/s). Samples were heat treated to the T6 condition and then subjected to 210 °C for 30 min prior to initiating the tests. Averaged results of the six tests are shown in Table 10. The results compare favorably with bulk material, with an average tensile failure strength of 184.1 MPa, versus 186.2 MPa for bulk material [20].

3.3 Fatigue Testing. To characterize the cyclic performance of the joints, room temperature fatigue testing was conducted on six samples that were heat treated to the T6 condition. An MTS 831 test frame was used to apply a cyclic load with a maximum stress of 32 ksi (220.63 MPa) and a minimum stress of 1.6 ksi (11.03 MPa), resulting in an R-ratio of + 0.05. The sinusoidal load was applied to the samples at 50 kHz until failure, and the number of cycles to failure was recorded for each test. The results of the testing are shown in Table 11. On average, the number of cycles to failure is approximately 190,000. Bulk aluminum material was tested under the same conditions, resulting in failure after 250,000 cycles. Published values for bulk aluminum 6061-T6 indicate failures after roughly 700,000 cycles [20] using cylindrical samples and similar test conditions.

4 Discussion

The DOE study found that lower scarf joint angles produce higher UTSs within the levels tested. Finite-element analysis indicates that higher relative displacements are occurring throughout the low angle joints. Because relative motion is the basis for ultrasonic joining, this likely produces the higher bond strength observed for lower angles.

Tensile tests on as-built scarf joint samples yielded an average tensile strength of 221.3 MPa, which is 29% lower than the UTS of bulk Al 6061-T6. Microsections of the joint do not indicate the presence of voids; therefore, other explanations for the decrease in strength are necessary. Aluminum 6061 is an age-hardenable material relying on solid solution and precipitation hardening as mechanisms for improving strength. During the ultrasonic joining process, the precipitates at the interface may be resolutionizing or migrating away from the interface, resulting in a decrease in strength. The strength of fully solutionized material is 241.3 MPa [13], on the same order as the as-built tests, supporting this hypothesis. Postprocess heat treatments have been successful in improving joint strength, indicating that the heat treatment is reintroducing precipitates at the interface that provide strength. To confirm this hypothesis, high-resolution microstructural evaluations, including nanoindentation at the joint interface, would be required.

High-temperature tensile tests showed that heat treated joints provide strengths similar to bulk material. This provides further evidence of the joint quality achievable using a postweld heat treatment. Similarly, the fatigue performance approaches that of bulk material with joint failures occurring after 190,000 cycles on average compared to bulk material failures after 250,000 cycles. These values are less than published bulk material results, which may be a result of differences in test specimen geometry. The rectangular shape of the specimens' cross sections can influence fatigue performance due to stress concentrations at sharp corners, which could be mitigated by using specimens with circular cross sections [21].

The use of UAM equipment in the nontraditional configuration presented here is an expansion of the capabilities of the technology. With UAM, multiple foils are typically built up to a desired dimension; however, the methodology presented here enables 0.076 in. (1.9304 mm) thick sheets to be joined with a single, flush weld joint, increasing the throughput. Using the joint configuration and concepts presented here, it may be possible to integrate the ultrasonic scarf joint concept with traditional UAM applications and other manufacturing methods to increase the speed and reduce the cost of part fabrication. For example, a part of a structure with embedded features such as cooling channels, sensors, electronics, or reinforcements could be built using UAM and then joined with sheets or parts produced using conventional processes.

Table 11 Cycles to failure for room temperature fatigue testing of six heat treated Al 6061-T6 joints

Sample	Avg. cycles to failure	SD
Heat treated	193,000	41,000

5 Summary

A methodology was developed for joining 0.076 in. (1.930 mm) thick aluminum 6061 sheets using ultrasonic welding. The approach uses UAM equipment as a means of creating ultrasonically welded seam joints. The flush joint design uses a scarf joint configuration and ultrasonic welding on both sides of the sheet to achieve a successful joint. A DOE study identified a 10 deg joint angle as the optimal geometry with an amplitude of 41 μm and weld speed of 25 in./min (10.58 mm/s) as optimal welding parameters within the range of parameter levels tested. Finite-element analysis indicates that lower angles produce superior bonds due to larger relative motions along the width of the joint surfaces. Resulting as-built joints yielded an average tensile strength of 221.3 MPa, which is 80.7 MPa less than that of the bulk material. Therefore, a heat treatment process was applied to the joints, resulting in an average room temperature tensile strength of 311 MPa, matching the bulk material. High-temperature tensile testing yielded an average strength of 184.1 MPa on average, similar to bulk material. Likewise, the cyclic fatigue behavior of the heat treated joints approaches that of bulk material.

Acknowledgment

The authors wish to acknowledge the member organizations of the Smart Vehicle Concepts Center, a National Science Foundation Industry/University Cooperative Research Center[2] established under NSF Grant No. IIP-1238286.

References

[1] Gould, J., 2012, "Joining Aluminum Sheet in the Automotive Industry—A 30 Year History," Weld. J., **91**, pp. 23–34.

[2] Melhem, G., Banyapadhyay, S., and Sorrell, C., 2014, "Use of Aerospace Fasteners in Mechanical and Structural Applications," Ann. Mater. Sci. Eng., **1**(4), pp. 1–5.

[3] Day, W., and Schwarzbach, J., 1946, "A Flight Investigation of the Effects of Surface Finish on Wing Profile Drag," J. Aeronaut. Sci., **13**(4), pp. 209–217.

[4] Dursun, T., and Soutis, C., 2014, "Recent Developments in Advanced Aircraft Aluminium Alloys," Mater. Des., **56**, pp. 862–871.

[5] Zhao, H., White, D., and DebRoy, T., 1999, "Current Issues and Problems in Laser Welding of Automotive Aluminium Alloys," Int. Mater. Rev., **44**(6), pp. 238–266.

[6] Collette, M., 2007, "The Impact of Fusion Welds on the Ultimate Strength of Aluminum Structures," 10th International Symposium on Practical Design of Ships and Other Floating Structures, Houston, TX, Oct. 4.

[7] Sriraman, M., Gonser, M., Fujii, H., Babu, S., and Bloss, M., 2011, "Thermal Transients During Processing of Materials by Very High Power Ultrasonic Additive Manufacturing," J. Mater. Process. Technol., **211**(10), pp. 1650–1657.

[8] Fujii, H., Sriraman, M., and Babu, S., 2011, "Quantitative Evaluation of Bulk and Interface Microstructures in Al-3003 Alloy Builds Made by Very High Power Ultrasonic Additive Manufacturing," Metall. Mater. Trans. A, **42**(13), pp. 4045–4055.

[9] Hansen, S., Vivek, A., and Daehn, G., 2015, "Impact Welding of Aluminum Alloys 6061 and 5052 by Vaporizing Foil Actuators: Heat-Affected Zone Size and Peel Strength," ASME J. Manuf. Sci. Eng., **137**(5), p. 051013.

[10] Lee, S., Kim, T., Hu, S., Cai, W., Abell, J., and Li, J., 2013, "Characterization of Joint Quality in Ultrasonic Welding of Battery Tabs," ASME J. Manuf. Sci. Eng., **135**(2), p. 021004.

[11] Lee, S., Kim, T., Hu, S., Cai, W., and Abell, J., 2015, "Analysis of Weld Formation in Multilayer Ultrasonic Metal Welding Using High-Speed Images," ASME J. Manuf. Sci. Eng., **137**(3), p. 031016.

[12] Graff, K., 2011, *Welding Fundamentals and Processes—Ultrasonic Additive Manufacturing*, Vol. 6A, ASM International, Materials Park, OH.

[13] ASM-International, 1992, *Properties of Wrought Aluminum and Aluminum Alloys—Properties and Selection: Nonferrous Alloys and Special-Purpose Materials*, Vol. 2, ASM International, Materials Park, OH.

[14] Tsujino, J., Ueoka, T., Kashino, T., and Sugahara, F., 2000, "Transverse and Torsional Complex Vibration Systems for Ultrasonic Seam Welding of Metal Plates," Ultrasonics, **38**(1–8), pp. 67–71.

[15] Wolcott, P., Hehr, A., and Dapino, M., 2014, "Optimized Welding Parameters for Al 6061 Ultrasonic Additive Manufactured Structures," J. Mater. Res., **29**(17), pp. 2055–2065.

[16] Hopkins, C., Fernandez, S., and Dapino, M., 2010, "Statistical Characterization of Ultrasonic Additive Manufacturing Ti/Al Composites," ASME J. Eng. Mater. Technol., **132**(4), p. 041006.

[17] Hopkins, C., Wolcott, P., Dapino, M., Truog, A., Babu, S., and Fernandez, S., 2012, "Optimizing Ultrasonic Additive Manufactured Al 3003 Properties With Statistical Modeling," ASME J. Eng. Mater. Technol., **134**(1), p. 011004.

[18] Dean, A., and Voss, D., 1999, *Design and Analysis of Experiments*, Springer, New York.

[19] ASM-International, 1991, *Heat Treating of Aluminum Alloys—Heat Treating*, Vol. 4, ASM-International, Materials Park, OH.

[20] Rice, R., Jackson, J., Bakuckas, J., and Thompson, S., 2011, *Metallic Materials Properties Development and Standardization*, Battelle Memorial Institute, Columbus, OH.

[21] Forrest, P., 1970, *Fatigue of Metals*, Pergamon Press, New York.

[2] www.SmartVehicleCenter.org